

# Current carrying blob-filaments and edge-localized-mode (ELM) dynamics

J. R. Myra

*Lodestar Research Corporation, Boulder, Colorado*

May 2007, Rev. Sept. 2007  
to be published in Phys. Plasmas

---

DOE/ER/54392-41

LRC-07-116

---

**LODESTAR RESEARCH CORPORATION**  
2400 Central Avenue  
Boulder, Colorado 80301

# **Current carrying blob-filaments and edge-localized-mode (ELM) dynamics**

J. R. Myra

*Lodestar Research Corp., 2400 Central Ave. P-5, Boulder, Colorado 80301*

## **Abstract**

The model of blob-filament propagation in the scrape-off-layer (SOL) of a tokamak is extended to include objects which carry a large net uni-directional current parallel to the magnetic field. Under experimentally realistic conditions, the blob-filament structure and propagation is influenced by magnetostatic forces. Some aspects of the model may be relevant to the SOL propagation of edge localized modes (ELMs).

PACS: 52.55.Fa, 52.25.Fi, 52.30.Cv, 52.40.Hf

## I. Introduction

Previous work by several authors has examined the theoretical properties of density (pressure) “blob” filaments.<sup>1-11</sup> The dynamics of these coherent structures, created by edge turbulence, is governed in part by dipole and higher-order parallel currents,  $\tilde{J}_{\parallel}$ . This “dipole” structure arises in the cross-section of the blob-filament in a plane perpendicular to the magnetic field, and is the result of charge separation by curvature and grad-B drift effects. In this paper, the model is extended by considering blob-filaments which also carry net (uni-directional, e.g. “monopole”) parallel current,  $\bar{J}_{\parallel}$ . The net current in the filament arises from the outward radial transport of parallel current carried by the tokamak during an edge localized mode (ELM) ejection event. The notion that current density, as well as particles and energy are lost from the main plasma in an ELM event has been proposed previously<sup>12</sup> and found to be consistent with experimental observations of strike-point jumps. Furthermore, direct observations of current carrying ELM filaments have been made in experiments conducted on the MegAmp Spherical Tokamak (MAST).<sup>13</sup> In the following, for brevity, the current carrying filamentary blobs will be referred to as ELMs, although the present model is not claimed to be a complete ELM model. In particular, this work emphasizes physics that is complementary to, but compatible with, the Alfvén wave dynamics of high beta blobs considered previously.<sup>4,6</sup>

The basic idea is that ELM pedestal instabilities are driven by a combination of edge current and pressure gradients.<sup>14</sup> Nonlinear saturation of these instabilities attempts to reduce the drives by removing filaments of plasma pressure and current, which propagate outward. Thus, it is postulated that each ELM filament carries with it the density, temperature, and *parallel current*<sup>12,13</sup> of the creation (instability) zone. This

current can interact with other currents through the  $\mathbf{J} \times \mathbf{B}$  force and thereby influence the dynamics.

The elementary result for the force per unit length between two long, parallel current carrying filaments is

$$F' = \frac{2I_1 I_2}{c^2 d} \rightarrow \frac{\mu_0 I_1 I_2}{2\pi d} \text{ (SI units)} \quad (1)$$

where  $I_1$  and  $I_2$  are the currents in the filaments and  $d$  is their perpendicular separation. Using an ELM-filament current illustrative of the MAST results<sup>13</sup> ( $I \sim 200$  A) and taking a parallel filament length  $L_{\parallel} \sim 1$  m, the total force is of order  $F = L_{\parallel} F' = 0.8/d(\text{cm})$  N. For comparison, the curvature force on a blob is  $F_{\kappa} = n m_i V 2c_s^2 / R$  where  $n$  is the blob density,  $m_i$  the ion mass,  $V = \pi \delta_b^2 L_{\parallel}$  the blob volume,  $\delta_b$  the blob radius,  $c_s$  the sound speed and  $R$  the major radius of the torus. Employing  $n = 10^{12} \text{ cm}^{-3}$ ,  $T_e = 50$  eV,  $\delta_b = 2$  cm,  $R = L_{\parallel} = 100$  cm, and  $\mu = 2$  (Deuterium) yields  $F_{\kappa} \sim 0.02$  N. Thus for reasonable perpendicular separations ( $d < 40$  cm) magnetostatic forces must be considered, in addition to the curvature effects which are known to induce radial blob (ELM) convection through curvature and grad-B-drift charge separation.

## II. Model equations

A simple model for current carrying ELM filaments result from the observation that in a sufficiently collisional scrape-off-layer (SOL) the parallel current convects with the density and temperature of the ELM. Considering time scales shorter than the time scale for parallel loss of the particles and energy in the filament, the ELM temperature  $T$  will be substantially larger than that of any surrounding background plasma. Thus the higher parallel electrical conductivity will confine the current to the location of the filament. We consider the lowest order  $\bar{E}_{\parallel} = E_0$  to be a spatially constant induction field, so that the spatial variation of (the lowest order)

$$\bar{J}_{\parallel} = E_0 / \eta_{\parallel} \quad (2)$$

is determined by  $T$  through the resistivity  $\eta_{\parallel} \sim T^{-3/2}$ . For simplicity in the following we take  $T = T(n)$  and therefore, the uni-directional component of the ELM current satisfies  $\bar{J}_{\parallel} = \bar{J}_{\parallel}(n)$ . If we can show that ELM-filament density and temperature convect across the SOL, then the preceding argument establishes (in an appropriate limit discussed subsequently) that the filamentary current will also be confined to, and convect with, the ELM.

The dynamics of these current-carrying ELM filaments can be studied in the reduced magneto-hydrodynamic (MHD) approximation, keeping the magnetostatic forces due to the current, as well as the usual curvature and grad-B forces that characterize electrostatic blob dynamics. Central to the model derivation is the standard vorticity equation

$$\nabla \cdot \frac{d}{dt} \left( \frac{nm_i c^2}{B^2} \nabla_{\perp} \Phi \right) = \nabla_{\parallel} J_{\parallel} + \frac{2c}{B} \mathbf{b} \times \kappa \cdot \nabla p \quad (3)$$

where  $d/dt = \partial/\partial t + \mathbf{v} \cdot \nabla$  and  $\mathbf{v} = (c/B)\mathbf{e}_z \times \nabla \Phi$ . Other notations have their usual meaning. In particular,  $n$  is the density,  $m_i$  is the ion mass,  $\Phi$  is the electrostatic potential,  $\mathbf{B}$  is the magnetic field,  $\mathbf{b} = \mathbf{B}/B$ ,  $\kappa \sim 1/R$  is the curvature, and  $p = nT$  is the electron pressure. For simplicity, to illustrate the basic idea, a cold ion model is considered, although retention of warm ion effects on the pressure, ion diamagnetic flows, and viscosity tensor would be more realistic.

To obtain a model set of dynamical equations for ELM-filament motion in the plane perpendicular to  $\mathbf{B}$ , it is necessary to derive a ‘‘closure’’ relation for the parallel current term in Eq. (3), relating it to dynamical quantities in the plane. For the well-studied<sup>1-11</sup> curvature driven electrostatic blobs, the parallel current acquires an approximately dipole structure, denoted  $\tilde{J}_{\parallel}$ , in the perpendicular plane as the result of charge separation by curvature and grad-B drift effects. The charge separation and

current flow pattern is illustrated in Fig. 1. Note that in addition to the dipole structure in the plane, these  $\tilde{J}_{\parallel}$  currents have an odd parity along the magnetic field (assuming the curvature source term is even at  $z = 0$ , the outboard midplane location). The parallel current  $\tilde{J}_{\parallel}$  flows in response to the charge pattern and completes a current loop which closes along the field lines, for example at their termination on divertor plates where sheath boundary conditions apply.<sup>1,2</sup>

For these odd-parity dipole parallel currents, the two-dimensional (2D) dynamics are well represented by integrating the vorticity equation along  $z$ , and retaining the sheath current term from the endpoint contributions.<sup>2</sup> More generally, an operator  $L(\Phi) \equiv [\tilde{J}_{\parallel}(z=+L_{\parallel}) - \tilde{J}_{\parallel}(z=-L_{\parallel})]/(2L_{\parallel})$  can be defined to describe the closure appropriate to a given set of boundary conditions along the field line. For example, in the sheath-connected limit<sup>1,2</sup>  $L(\Phi) \approx 2ne^2c_s(\Phi - \Phi_f)/(L_{\parallel}T)$  where  $\Phi_f \approx 3T/e$  is the floating potential. Also relevant to high-beta ELMs is closure by Alfvén wave emission along the magnetic field<sup>4-6,15</sup> where bending of the field lines occurs due to the dipole current. This high-beta closure (also called the RX-EM regime in Ref. 5) is  $L(\Phi) \approx -2c^2/(4\pi v_{a0}L_{\parallel})\nabla_{\perp}^2\Phi$  where  $v_{a0}$  is based on the background ambient density  $n_0$ . Some additional examples of closure relations are discussed in Refs. 5 and 10.

The point of the present paper is to include the effects on the 2D dynamics of an additional uni-directional (e.g. monopole) current [see Fig 1b)] carried by the ELM filament. In order to assess the magneto-static forces arising from this ELM current, it is crucial to distinguish between the equilibrium background field  $\mathbf{B}$ , and self-consistent (ELM generated) fields. A slab model is considered where the equilibrium field is straight,  $\mathbf{e}_z = \mathbf{B}/B$  is the unit vector along the *equilibrium* magnetic field, and the notation  $\parallel$  refers to the total magnetic field  $\mathbf{B} - \mathbf{e}_z \times \nabla \bar{A}_z$  where the self-generated magnetic field due to the ELM current  $\bar{J}_z$  is described by  $\bar{A}_z$ . The field-line averaging of the vorticity equation proceeds by employing

$$\mathbf{J}_z = \tilde{\mathbf{J}}_z + \bar{\mathbf{J}}_z \quad (4)$$

and  $\nabla_{\parallel} = \mathbf{e}_z \cdot \nabla - (1/B) \mathbf{e}_z \cdot \nabla A_z \times \nabla$ . Taking  $\nabla_{\parallel} \mathbf{J}_{\parallel} \approx \nabla_{\parallel} \mathbf{J}_z$ , the field line average of the  $d\tilde{\mathbf{J}}_z/dz$  term yields the L operator introduced previously. Making the simplifying assumption that  $\bar{\mathbf{J}}_z$  is constant along B, the  $d\bar{\mathbf{J}}_z/dz$  term makes no contribution to the field-line averaged equation, and the new terms all arise from  $\mathbf{e}_z \cdot \nabla A_z \times \nabla \mathbf{J}_z$ , which is just the reduced MHD magnetostatic force contribution. The sub-ordering,  $\tilde{\mathbf{J}}_z \ll \bar{\mathbf{J}}_z$ , invoked next, highlights the effects of the ELM current, and gives rise to the following set of field-line-averaged model equations

$$\frac{c^2}{4\pi v_a^2} \frac{d}{dt} \nabla_{\perp}^2 \Phi - L(\Phi) = \frac{2c}{B} \mathbf{e}_z \times \kappa \cdot \nabla p + \frac{1}{B} \mathbf{e}_z \cdot \nabla \bar{\mathbf{J}}_z \times \nabla \bar{A}_z \quad (5)$$

$$\frac{dn}{dt} = 0 \quad (6)$$

$$\nabla_{\perp}^2 \bar{A}_z = -\frac{4\pi}{c} \bar{\mathbf{J}}_z \quad (7)$$

where, in Eq. (5),  $v_a$  is the Alfvén velocity, and the non-essential but usual Boussinesque approximation has been made for the vorticity advection term on the left. Here  $\kappa$  now refers to an appropriate field-line-averaged curvature.

From the derivation and discussion, it should be clear that the descriptive terms “monopole” and “dipole” are used somewhat loosely in this paper to indicate the sign and character of current flow (net vs. cancelling). They describe the lowest order multipole contributions to the current that contribute to the physics of magnetostatic forcing and charge-separation-induced convection, respectively, in the 2D plane. The model itself applies to any function  $\bar{\mathbf{J}}_z(x, y)$  that is constant along  $z$ ; and the usual closure relations assume only that  $\tilde{\mathbf{J}}_z(x, y)$  is odd in  $z$ .

The model equations neglect dipole-current contributions to the magnetostatic force, e.g.  $\mathbf{e}_z \cdot \nabla \tilde{\mathbf{J}}_z \times \nabla \bar{A}_z$ , and the fact that the ELM currents flow on bent field lines  $\mathbf{e}_z \cdot \nabla \bar{\mathbf{J}}_z \times \nabla \bar{A}_z$ . These effects are regarded as less important here because the dipole

fields fall off rapidly in space in the x-y plane as one moves away from the ELM, and also these particular terms have an odd parity along B which makes their field-line-averaged contribution small.

As an aside, note that the  $\mathbf{e}_z \cdot \nabla \tilde{J}_z \times \nabla \bar{A}_z$  term describes the effect of local rotational transform due to the ELM current on the (dipole curvature-induced) polarization charges. If strong enough, this effect can mitigate charge polarization and hence slow the radial convective velocity. However, for  $J_b \sim J_{\text{edge}}$  (where  $J_b$  is the blob/ELM current) this effect will not be qualitatively important while the ELM filament is localized to the outboard midplane, since  $J_{\text{edge}} \sim B_\theta/r$  and  $J_b \sim B_{\theta b}/\delta_b$  gives  $q_b \sim q_{\text{edge}}$  where  $q_{\text{edge}}$  is the usual safety factor and  $q_b = \delta_b B/RB_{\theta b}$ , i.e. the local rotational transform due to the ELM current is the same order as that due to background field.

In general, Eq. (2) should be replaced by a more complete Ohm's law

$$\frac{1}{c} \frac{d\bar{A}_z}{dt} + \frac{\Delta\Phi}{L_{\parallel}} = E_0 - \eta_z \bar{J}_z \quad (8)$$

where  $\Delta\Phi$  is any net floating potential difference along the field-line segment, e.g. plate-to-plate for a sheath-connected filament. The time scale for ELM convection  $\tau_b \sim \delta_b/v_{\perp}$  is normally short compared to the resistive diffusion time inside the filament where T is relatively high,  $\tau_{\eta} = 4\pi\delta_b^2/(\eta_{\parallel}c^2)$ , suggesting the retention of  $d\bar{A}_z/dt$ . In addition, electron inertial effects should be added to Eq. (8) when  $\delta_b < c/\omega_{pe}$ . However, for a coherent propagating ELM that retains its structure, e.g. a ‘‘blob’’ solution,<sup>1,2</sup> the time derivative of the structure ideally vanishes in the moving frame so that  $d\bar{A}_z/dt \approx d\bar{J}_z/dt \approx dn/dt \approx dT/dt \approx 0$ . In practice, electrostatic blob simulations (see e.g. Refs. 4-6) show that  $dn/dt$  is not strictly zero in the blob frame; instead, slow evolution (relative to  $\tau_b$ ) of the structure occurs. Thus the simplest justification for employing Eq. (2) in place of Eq. (8) is the rather harsh restriction  $\tau_{\eta} \ll \tau_b$ . In the present model, however, it will be seen subsequently that the magnetostatic force term itself acts to retain coherency of a

circular-cross-section ELM-blob structure, so a broader validity condition is expected to pertain. Further attention to this issue, likely requiring numerical simulation, will be deferred to a later investigation.

From Ampere's law, for two ELMs of perpendicular radius  $\delta_b$ , separated by  $d$ , we estimate  $\nabla_{\perp} \bar{A}_z \sim 2\pi \bar{J}_z \delta_b^2/dc$ . The magneto-static force from the last term of Eq. (5) provides an acceleration term (which may lead to steady blob velocity or not, depending on the regime and transient or steady conditions) that can be estimated from  $v \sim (c\Phi/\delta_b B)$  and Eq. (5) as

$$\dot{v} = \frac{8\pi^2 v_a^2 \delta_b^2 \bar{J}_z^2}{c^2 B^2 d} \quad (9)$$

In dimensionless ratio form (to the Bohm scales for time =  $1/\Omega_i$  and space =  $\rho_s = c_s/\Omega_i$ ) this yields

$$\frac{\dot{v}}{\Omega_i c_s} = \frac{4\rho_s}{\beta_{bi} d} \quad (10)$$

where an ‘‘internal’’ blob (ELM) beta has been defined as

$$\beta_{bi} = \frac{8\pi n T_e}{B_{bi}^2} = 8\pi n T_e \left( \frac{\delta_b c}{2I} \right)^2 \quad (11)$$

Here, the current carried by the filament is  $I = \bar{J}_z \pi \delta_b^2$  and  $B_{bi}$  is the magnetic field from this current at one blob radius. An estimate for the strength of the curvature term in Eq. (5) yields

$$\frac{\dot{v}_{\kappa}}{\Omega_i c_s} = \frac{2\rho_s}{R} \quad (12)$$

Comparing Eqs. (10) and (12) shows that magnetostatic forces will dominate the curvature-induced forces on an ELM when  $\beta_{bi} d < 2R$ . For the parameters given earlier, we estimate  $\beta_{bi} \sim 5 - 10$  (depending on whether we include the ion pressure which is technically zero in the rudimentary model equations).

### III. Magnetostatic force effects on ELM-filament dynamics

The effect of the magnetostatic force term on ELM dynamics is considered next. For an *isolated* cylindrically-symmetric current filament we have  $\bar{\mathbf{J}}_z = \bar{\mathbf{J}}_z(r)$ ,  $\bar{\mathbf{A}}_z = \bar{\mathbf{A}}_z(r)$  (where  $r = 0$  is the filament's center) and the force vanishes,  $\mathbf{e}_z \cdot \nabla \bar{\mathbf{J}}_z \times \nabla \bar{\mathbf{A}}_z = 0$ . This leads to the first important conclusion: *an isolated current carrying ELM filament experiences the same curvature-driven outward radial convection as its current-free blob counterpart.*<sup>1-11</sup> This convection velocity is estimated as  $v_x \sim c\Phi/(\delta_b B)$  where, from Eq. (5),  $\Phi$  is obtained by balancing the curvature term with the dominant term on the left-hand-side. For the sheath-connected limit, this yields the familiar<sup>1,2</sup> result  $v_x \sim c_s(L_{\parallel}/R)(\rho_s/\delta_b)^2$ . Indeed the observed radial convection velocity of ELMs is roughly consistent with blob-based estimates.<sup>16-18</sup>

More generally, the magnetostatic term will act on structures with asymmetric current, and will cause two ELMs (which have the same direction of current filaments) to be attracted, and possibly merge. This is just the result of the current pinch: the attractive force will tend to symmetrize any localized structure in the 2D plane, evolving it to a cylindrically symmetric filament. As the symmetrization progresses, the bulk (e.g. center of mass) motion of the ELM is expected to convect roughly at the rate derived in the preceding for the cylindrically symmetric case.

The attractive current-pinch force will also mitigate the blob bifurcation and fingering instabilities that occur in the electrostatic case.<sup>19,20</sup> Additional calculations, not reported on in detail here, show that the stability problem for an isolated circularly-symmetric 2D ELM is closely related to the classical rippling mode calculations.<sup>21,22</sup> In a local slab approximation (valid for high-mode number perturbations of the ELM filament) neglecting curvature, retaining  $\nabla_z \bar{\mathbf{J}}_z$  in the vorticity equation and employing the full Ohm's law [Eq. (8) with  $\Delta\Phi/L_{\parallel} \rightarrow \nabla_z \Phi$ ], the dispersion relation is

$$1 - \frac{i\gamma_{\text{rip}}}{\omega} = \frac{\omega(\omega + i\omega_\eta)}{\omega_a^2} \quad (13)$$

where

$$\gamma_{\text{rip}} \equiv -\frac{\bar{J}_z \eta'_z k_y c}{k_{\parallel} B} \quad (14)$$

$\omega_\eta = \eta_z k_{\perp}^2 c^2 / 4\pi$ ,  $k_{\parallel} = k_z + k_\theta B_\theta / B_z$ ,  $' = d/dr$  and  $(r, \theta)$  are cylindrical coordinates based on the symmetry axis of the filament. Note that  $\eta'_z > 0$  for T decaying away from the filament's center, and that  $\bar{J}_z$  and  $B_\theta$  carry the same sign. The electrostatic rippling mode corresponds to the limit where the rhs of Eq. (13) is negligible, resulting in  $\omega = i\gamma_{\text{rip}}$  and yielding instability if  $\gamma_{\text{rip}} > 0$ . For general  $(k_z, k_\theta)$  this is possible, however in the 2D context where  $k_z = 0$ , we have  $\bar{J}_z k_y / k_{\parallel} > 0$  and the mode is stable (actually damped). Other branches are also stable because  $\omega_\eta / \gamma_{\text{rip}} \sim k_{\perp}^2 \delta_b^2 \gg 1$  in local theory. For “global” low- $m$  (relative to the filament) modes, we can consider electromagnetic kink-type perturbations. If the ELM  $\bar{J}_z$  is smaller than that of the edge plasma and  $q_{\text{edge}} \gg 1$ , kinks are normally stable, even when finite  $k_z$  is allowed. For perturbations confined to the 2D plane, the magnetostatic terms provide over-stability for  $m > 1$  (i.e.  $\omega^2 \approx k_{\parallel}^2 v_a^2 \approx k_y^2 B_\theta^2 v_a^2 / B^2 > 0$  where  $k_y \sim m / \delta_b$ ), and should thus give a stabilizing contribution to curvature-driven modes. This contribution is important when  $k_y^2 R \delta_b > \beta_{\text{bi}}$  which is easy to satisfy.

Thus the stability of an isolated ELM in the 2D model is enhanced over its current-free blob counterpart due to the magnetostatic current pinch, which will tend to circularize the object in the 2D plane, enhancing its coherency as it propagates. Consequently, as alluded to following Eq. (8), the validity of neglecting  $d/dt$  in the ELM frame should also be enhanced relative to the electrostatic blob case.

The interaction of an ELM filament with the edge plasma and wall, is also an interesting aspect of the model. Consider first the formation of an ELM. The postulate,

(see the Introduction) is that during an ELM event current density, as well as particles and energy, are lost from the main plasma, i.e. each ELM filament carries with it the density, temperature, and *parallel current* of the creation (peeling-ballooning instability) zone. A “force-free”  $\bar{J}_z$ -carrying ELM filament does not interact with the equilibrium magnetic field  $\mathbf{B} = B\mathbf{e}_z$ . But, because the total current carried by the torus is conserved on short time scales, the ejected ELM-filament must leave behind a “current-hole” in the creation zone, i.e. a region depleted of current just as it is depleted of pressure (see Fig. 2 inset). This region of depleted current can be modeled heuristically as the original equilibrium plus an oppositely signed localized current filament.

Consider the current filament-hole pair in the left part of Fig. 2. As long as the current-hole exists, it will exert a repulsive force on the ELM (because the hole and ELM have oppositely-directed  $\bar{J}_z$  currents), thus the ELM will be accelerated into the SOL. [This magnetostatic current repulsion is clearly a different mechanism than that which gives rise to “explosive” pressure-gradient-driven ballooning<sup>23</sup> although the result on the emerging ELM is qualitatively similar.] After a characteristic healing time for the main plasma (e.g. due to turbulence and parallel flows of particles and current which act to restore pressure and current to flux functions), the magnetostatic force on the ejected ELM will again vanish (as in the isolated ELM case discussed previously) since the interaction of the main tokamak magnetic field with a purely parallel current is force-free. However, the curvature-induced radial convection remains.

Fig. 2 also depicts (at right) an ELM approaching a perfectly conducting wall. In order to make the normal component of  $\mathbf{B}$  vanish at the wall, the parallel current in the image flows in the opposite direction. Thus the blob will be repelled by the wall (flux compression of the ELM’s magnetic-field against the wall), causing its radial motion to decelerate. For resistive walls there is an additional effect: deceleration of the toroidal

rotation of the blob due to image currents. Such toroidal deceleration has been observed.<sup>13</sup>

#### **IV. Conclusion**

In conclusion, a model for 2D ELM dynamics that includes net uni-directional current flow along the filament, appears to be both feasible and interesting. The model suggests that an ELM will be accelerated away from the plasma, near the edge, (due to interaction with its hole pair) then (after the hole heals) drift with a constant  $\mathbf{E} \times \mathbf{B}$  drift in the curvature-dominated zone for isolated ELM filaments, and finally decelerate close to the wall, *assuming it maintains its parallel current  $\bar{J}_z$  and temperature  $T$  as it convects*. More realistically, some  $\bar{J}_z$  and  $T$  convected by the ELM could be lost to sheaths by the time the ELM reaches the wall, mitigating the image current deceleration effect in some cases. The current carried by the ELM enhances coherency (secondary stability) in the perpendicular plane, but allow resistive rippling and other instabilities in 3D.

*note added in proof:* Recent nonlinear MHD simulations of ELMs<sup>24–29</sup> show filament formation. In particular, Ref. 24 explicitly discusses the observation of ELM filaments which carry current. Field-aligned holes left behind after filament ejection have been reported in recent experiments.<sup>30</sup>

#### **Acknowledgments**

The author thanks D. A. D’Ippolito for useful discussions and a critical reading of the manuscript. This work was supported by the U.S. Department of Energy (DOE) under grant DE-FG02-97ER54392; however, such support does not constitute an endorsement by the DOE of the views expressed herein.

## References

- <sup>1</sup> S. I. Krasheninnikov, Phys. Lett. A **283**, 368 (2001).
- <sup>2</sup> D. A. D'Ippolito, J. R. Myra and S. I. Krasheninnikov, Phys. Plasmas **9**, 222 (2002).
- <sup>3</sup> N. Bian, S. Benkadda, J.-V. Paulsen, and O. E. Garcia, Phys. Plasmas **10**, 671 (2003).
- <sup>4</sup> S. I. Krasheninnikov, D. D. Ryutov, and G. Yu, J. Plasma Fusion Res. **6**, 139 (2004).
- <sup>5</sup> J. R. Myra and D. A. D'Ippolito, Phys. Plasmas **12**, 092511 (2005).
- <sup>6</sup> G. Q. Yu, S. I. Krasheninnikov and P.N. Guzdar, Phys. Plasmas **13**, 042508 (2006).
- <sup>7</sup> O. Garcia, V. Naulin, A. H. Nielsen, and J. Juul Rasmussen, Phys. Plasmas **12**, 062309 (2005)
- <sup>8</sup> D. D. Ryutov, Phys. Plasmas **13**, 122307 (2006).
- <sup>9</sup> R. H. Cohen and D. D. Ryutov, Contrib. Plasma Phys. **46**, 678 (2006).
- <sup>10</sup> S. I. Krasheninnikov, A. I. Smolyakov, G. Yu, and T. K. Soboleva, Czech. J. of Phys. **55**, 307 (2005).
- <sup>11</sup> J. R. Myra, D. A. Russell, and D. A. D'Ippolito, Phys. Plasmas **13**, 112502 (2006).
- <sup>12</sup> E. R. Solano, S. Jachmich, F. Villone, N. Hawkes, *et al.*, J. Nucl. Mater. 337–339, 747 (2005); E. R. Solano, S. Jachmich, F. Villone, N. Hawkes, *et al.*, in *Proceedings of the 20th IAEA Fusion Energy Conference*, 1 - 6 November 2004, Vilamoura, Portugal (IAEA, Vienna, 2005), paper IAEA-CN-116/EX/P1-3.
- <sup>13</sup> A. Kirk, N. B. Ayed, G. Counsell, B. Dudson. *et al.*, Plasma Phys. Control. Fusion **48**, B433 (2006).
- <sup>14</sup> P. B. Snyder, H. R. Wilson, J. R. Ferron, L. L. Lao, *et al.*, Phys. Plasmas **9**, 2037 (2002).
- <sup>15</sup> P.B. Parks, W.D. Sessions and L.R. Baylor, Phys. Plasmas **7**, 1968 (2000).
- <sup>16</sup> W. Fundamenski, W. Sailer and JET EFDA contributors, Plasma Phys. Control. Fusion **46**, 233 (2004).

- <sup>17</sup> D.L. Rudakov, J.A. Boedo, R.A. Moyer, P.C. Stangeby, *et al.*, Nucl. Fusion **45**, 1589 (2005).
- <sup>18</sup> J.A. Boedo, R.J. Maqueda, D.L. Rudakov, G.R. McKee, *et al.*, “Particle and Energy Transport in the SOL of DIII-D and NSTX”, in *Proceedings of the 21st IAEA Fusion Energy Conference*, 16 - 21 October 2006, Chengdu, (IAEA, Vienna, 2006), paper IAEA-CN-149/EX/P4-2; submitted to Nucl. Fusion (2007).
- <sup>19</sup> D. A. D’Ippolito and J. R. Myra, Phys. Plasmas **10**, 4029 (2003).
- <sup>20</sup> G. Q. Yu and S. I. Krasheninnikov, Phys. Plasmas **10**, 4413 (2003).
- <sup>21</sup> H.B. Furth, J. Killeen and M. N. Rosenbluth, Phys. Fluids **6**, 459 (1963).
- <sup>22</sup> see e.g. B.A. Carreras, P.W. Gaffney, H. R. Hicks, and J. D. Callen, Phys. Fluids **28**, 1231 (1982) for a treatment that is close to the present formulation.
- <sup>23</sup> H.R. Wilson and S.C. Cowley, Phys. Rev. Lett. **92**, 175006 (2004).
- <sup>24</sup> G.T.A. Huysmans and O. Czarny, Nucl. Fusion **47**, 659 (2007).
- <sup>25</sup> N. Mizuguchi, R. Khan, T. Hayashi and N. Nakajima, Nucl. Fusion **47**, 579 (2007).
- <sup>26</sup> R. Khan, N. Mizuguchi, N. Nakajima, and T. Hayashi, Phys. Plasmas **14**, 062302 (2007).
- <sup>27</sup> P.B. Snyder, H.R. Wilson and X.Q. Xu, Phys. Plasmas **12**, 056115 (2005).
- <sup>28</sup> C.R. Sovinec, D.D. Schnack, A.Y. Pankin, *et al.*, J. Phys.: Conf. Ser. **16**, 25 (2005).
- <sup>29</sup> H.R. Strauss, L. Sugiyama, C.S. Chang *et al.*, Proc. 21st Int. Conf. on Fusion Energy, Chengdu (IAEA, Vienna, 2006) CD-ROM file TH/P8-6.
- <sup>30</sup> R. Scannell, A. Kirk, N. Ben Ayed, P.G. Carolan, *et al.*, Plasma Phys. Control. Fusion **49**, 1431 (2007); B. Kurzan, H. D. Murmann, and J. Neuhauser, Phys. Rev. Lett. **95**, 145001 (2005).

## Figure captions

1. Sketch of current flow in blob and ELM filaments (cutaway view): a) charge separation due to a gravity force  $\mathbf{g}$  (e.g. from curvature), resulting “dipole” parallel current pattern, and  $\mathbf{E} \times \mathbf{B}$  convection; b) additional unidirectional (“monopole”) current flow in an ELM filament.
2. Sketch of interactions of a current-carrying blob (ELM) with its creation-hole, (left) and with a wall (right). The direction of parallel current flow is indicated by the cross and dot symbols. The force with the image or hole is repulsive in both cases. Inset at upper left: Peeling-ballooning instability is postulated to deform the radial current profile in the plasma creating the ELM-hole pair.

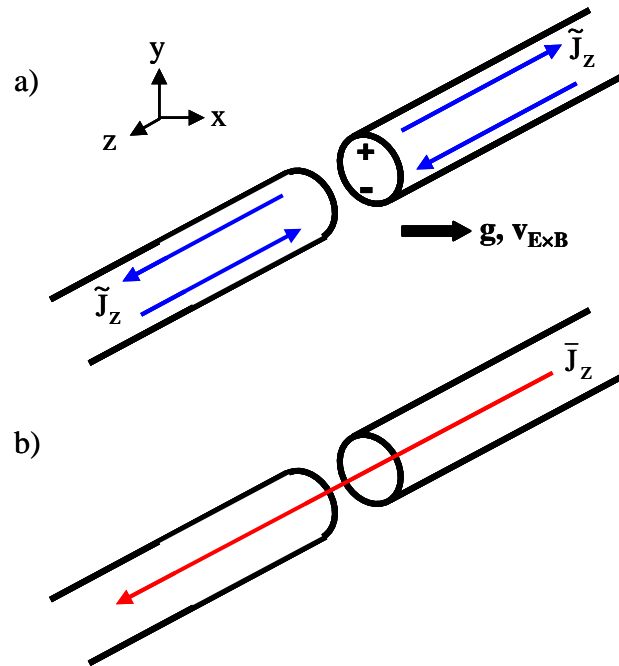


Fig. 1 Sketch of current flow in blob and ELM filaments (cutaway view): a) charge separation due to a gravity force  $\mathbf{g}$  (e.g. from curvature), resulting “dipole” parallel current pattern, and  $E \times B$  convection; b) additional unidirectional (“monopole”) current flow in an ELM filament.

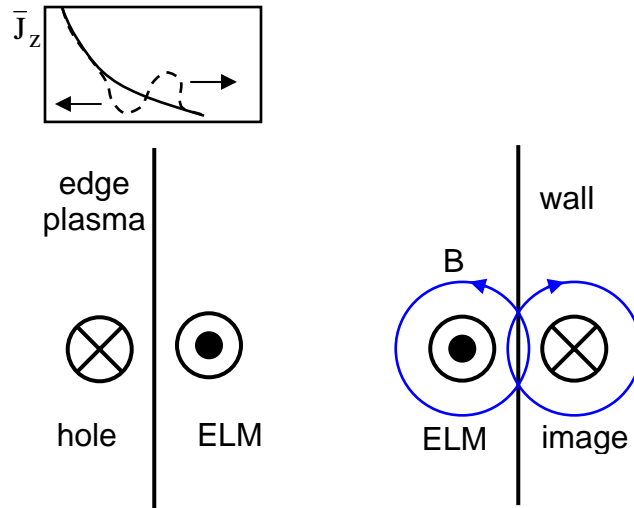


Fig. 2 Sketch of interactions of a current-carrying blob (ELM) with its creation-hole, (left) and with a wall (right). The direction of parallel current flow is indicated by the cross and dot symbols. The force with the image or hole is repulsive in both cases. Inset at upper left: Peeling-ballooning instability is postulated to deform the radial current profile in the plasma creating the ELM-hole pair.